

Mutant α -Latrotoxin (LTX^{N4C}) Does Not Form Pores and Causes Secretion by Receptor Stimulation

THIS ACTION DOES NOT REQUIRE NEUREXINS*

Received for publication, October 10, 2002, and in revised form, May 19, 2003
Published, JBC Papers in Press, June 2, 2003, DOI 10.1074/jbc.M210395200

Kirill E. Volynski[‡], Marco Capogna[§], Anthony C. Ashton[‡], Derek Thomson[¶], Elena V. Orlova[‡],
Catherine F. Manser[‡], Richard R. Ribchester[¶], and Yuri A. Ushkaryov^{‡**}

From the [‡]Department of Biological Sciences, Imperial College London, London SW7 2AY, United Kingdom, the [§]Medical Research Council, Anatomical Neuropharmacology Unit, Oxford OX1 3TH, United Kingdom, and the [¶]Department of Neuroscience, University of Edinburgh, Edinburgh EH8 9JZ, United Kingdom

α -Latrotoxin (LTX) causes massive release of neurotransmitters via a complex mechanism involving (i) activation of receptor(s) and (ii) toxin insertion into the plasma membrane with (iii) subsequent pore formation. Using cryo-electron microscopy, electrophysiological and biochemical methods, we demonstrate here that the recently described toxin mutant (LTX^{N4C}) is unable to insert into membranes and form pores due to its inability to assemble into tetramers. However, this mutant still binds to major LTX receptors (latrophilin and neurexin) and causes strong transmitter exocytosis in synaptosomes, hippocampal slice cultures, neuromuscular junctions, and chromaffin cells. In the absence of mutant incorporation into the membrane, receptor activation must be the only mechanism by which LTX^{N4C} triggers exocytosis. An interesting feature of this receptor-mediated transmitter release is its dependence on extracellular Ca²⁺. Because Ca²⁺ is also strictly required for LTX interaction with neurexin, the latter might be the only receptor mediating the LTX^{N4C} action. To test this hypothesis, we used conditions (substitution of Ca²⁺ in the medium with Sr²⁺) under which LTX^{N4C} does not bind to any member of the neurexin family but still interacts with latrophilin. We show that, in all the systems tested, Sr²⁺ fully replaces Ca²⁺ in supporting the stimulatory effect of LTX^{N4C}. These results indicate that LTX^{N4C} can cause neurotransmitter release just by stimulating a receptor and that neurexins are not critical for this receptor-mediated action.

α -Latrotoxin (LTX)¹ stimulates exhaustive release of neurotransmitters in vertebrates. This toxin has been extensively used to probe molecular mechanisms that control exocytosis of both synaptic vesicles (SVs) and large dense-core vesicles (LD-

CVs) in such diverse models as brain, neuromuscular junctions, and endocrine cells (for reviews see Refs. 1–3).

LTX acts only after binding to presynaptic receptors (4). Once receptor-bound, the toxin can trigger exocytosis by several mechanisms: (i) activation of the receptors (5–8), (ii) formation of non-selective pores in the membrane (9–11), and (iii) hypothetical intracellular interaction with the exocytotic machinery (12).

Because toxin pores damage cell membranes and produce strong cytotoxic effects (*e.g.* 13–15), only the receptor-transduced LTX action is likely to reveal intact, physiologically important exocytotic mechanisms. Unfortunately, this action is difficult to study using the wild-type LTX (LTX^{WT}) because it easily inserts into membranes and forms ionic pores (9–11, 16). This problem could be overcome by designing LTX mutants that would lack the propensity of membrane insertion, and a promising toxin variant has been described recently (LTX^{N4C}) (17). This mutant had the same affinity for the receptors as LTX^{WT} (17) but failed to form pores in synaptosomes or receptor-transfected BHK cells (8). Lacking the major (ionophore) activity, LTX^{N4C} was originally thought to be altogether inactive (12, 17). However, we have discovered that, in fact, LTX^{N4C} strongly stimulates receptor-mediated transmitter release (8), providing an ideal tool for investigating exocytotic signals transduced by LTX receptors.

If LTX^{N4C} acts via receptor stimulation, which LTX receptor is crucial for this signaling? Two major receptors have been isolated that bind LTX specifically and with high affinities: neurexin I α (NRX I α) (18) and latrophilin 1 (LPH, also called CIRL) (19, 20). NRXs are a family of single-pass transmembrane proteins that resemble cell-contact molecules (18). There are three long (α) and three short (β) forms of NRXs transcribed from three homologous genes (18, 21). While NRX I α binds LTX strongly, other homologs have low affinities for the toxin (22); however, all NRXs strictly require Ca²⁺ for this interaction (22, 23). LPH is a G protein-coupled receptor that binds LTX avidly under all ionic conditions (5). LPH also has two homologs (LPH 2 and 3), but these do not interact with LTX appreciably (22, 24, 25).

Interestingly, the receptor-mediated effect of LTX^{N4C} in central synapses is Ca²⁺-dependent (8), reasonably suggesting that the Ca²⁺-dependent receptors (*i.e.* NRXs) may be responsible for mediating this LTX action. Although this hypothesis contradicted our previous results (5, 26, 27), we decided to test it using the fact that Sr²⁺ does not support the interaction of LTX with NRX I α but substitutes Ca²⁺ in LTX-evoked exocytosis (5).

The objectives of the current study were (i) to reveal the

* This work was supported by the Wellcome Trust (Senior European Research Fellowship (to Y. A. U.)), project grant (to R. R. R.), Medical Research Council (to M. C.), and Biotechnology and Biological Sciences Research Council (Research Grant 28/B14085 (to Y. A. U.)). The costs of publication of this article were defrayed in part by the payment of page charges. This article must therefore be hereby marked "advertisement" in accordance with 18 U.S.C. Section 1734 solely to indicate this fact.

¶ Current address: Dept. of Crystallography, Birkbeck College, London WC1E 7HX, UK.

** To whom correspondence should be addressed. Tel.: 44-(0)20-7594-5237; Fax: 44-(0)20-7594-5207; E-mail: y.ushkaryov@imperial.ac.uk.

¹ The abbreviations used are: LTX, α -latrotoxin; LDCV, large dense-core vesicles; LPH, latrophilin; LTX^{NAT}, native LTX; LTX^{N4C}, mutant LTX; LTX^{WT}, wild-type LTX; mepps, miniature end-plate potentials; mEPSCs, miniature excitatory postsynaptic currents; NMJ, neuromuscular junction; NRX, neurexin; Ab, antibody; SVs, synaptic vesicles.

molecular basis of the mutant's inability to form ionic pores and (ii) to assess the importance of NRX(s) for the receptor-mediated LTX action. We show that LTX^{N4C} is unable to form pores because it fails to assemble into tetramers. In several model systems that endogenously express both LPH and NRXs (rat synaptosomes; rat hippocampal cultures; mouse neuromuscular junctions, NMJs; and bovine chromaffin cells), we demonstrate that, in the presence of Sr²⁺, LTX^{N4C} does not interact with any NRX, but still strongly stimulates receptor-mediated neurotransmitter release. We conclude that NRXs are not strictly required for the receptor-transduced LTX signaling and suggest that LPH is the major player in this process.

EXPERIMENTAL PROCEDURES

Materials—Native toxin (LTX^{NAT}) was purified from the black widow spider venom as described (16). Monoclonal antibody (mAb) A15 against LTX was a kind gift from Prof. E. V. Grishin. A polyclonal anti-LTX Ab was obtained by immunizing rabbits with SDS-denatured LTX. A rabbit Ab recognizing the C termini of NRXs and a rabbit Ab against the extracellular domain of LPH were described in Ref. 9.

Production and Purification of Recombinant Toxins—The construction of baculovirus for LTX^{WT} expression was outlined previously (28). The cDNA encoding LTX^{N4C} (17) was combined from two fragments obtained by polymerase chain reactions on the LTX^{WT} template between the following primer pairs: 5'-TTGGGATCCGAAGGAGAAGATTTAACT/5'-TGTCGCCTCGAGGTACTAGGTATGGTGTGATTTTC and 5'-AAATCGTACCTCGAGGATCAAATTTTCATCGACATT/5'-GAACTCTCGAGTTACCTCCGAAATTTTCGCT. These fragments were consecutively ligated into the baculovirus transfer vector pMelBacA (Invitrogen). The final LTX^{N4C} construct was verified by complete sequencing and co-transfected with the viral DNA (Bac-N-Blue kit, Invitrogen) into Sf9 cells cultured in complete TNM-FH medium (Invitrogen). Positive plaque selection, production of high-titer baculovirus stocks and large-scale expression of recombinant toxins in Hi5 cells was carried out as published (28).

Recombinant toxins were purified by affinity chromatography on the A15 mAb attached to CNBr-activated Sepharose (Amersham Biosciences). For this purpose, expression medium containing a secreted recombinant LTX was filtered through a 0.22 μ m filter (Whatman) and then passed through the antibody column. The column was washed with 150 mM NaCl, 50 mM Tris-HCl, pH 8.2, and eluted with three column volumes of 1 M MgCl₂, 50 mM Tris-HCl, pH 8.2. Chromatographic fractions were analyzed by SDS-electrophoresis/Western blotting, and those containing the recombinant LTXs were pooled, dialyzed against TBSM (in mM: 150 NaCl, 2.0 MgCl₂, 50 Tris-HCl; pH 8.2) and concentrated in a Vivaspine6 unit (Sartorius) to ~50 nM.

Channel/Pore Formation by Recombinant Toxins—Constructs for expression of LPH and NRX have been described previously (9). To measure ⁴⁵Ca²⁺ influx, COS7 cells were transfected with LPH or NRX I α (9) and plated onto 12-well culture plates at 40% confluence. One day after transfection, the cells were incubated with different concentrations of recombinant toxins in buffer A (in mM: 145 NaCl, 5.6 KCl, 5.6 glucose, 0.5 MgCl₂, 15 HEPES, and 0.5 mg/ml bovine serum albumin; pH 7.4) supplemented with 2 mM CaCl₂ and 10 μ Ci/ml of ⁴⁵Ca²⁺. After 5 min incubation, the medium was removed, and the cells washed twice. The amount of radioactivity accumulated by cells was determined by liquid scintillation counting of cells solubilized in 1% Triton X-100.

For electrophysiological detection of toxin channels, CHO cells, maintained in Dulbecco's modified Eagle's medium supplemented with 10% heat-inactivated fetal bovine serum and antibiotics (Invitrogen), were transiently co-transfected with receptor constructs mixed with pEGFP-N2 (Clontech) encoding green fluorescent protein (to identify transfected cells); FUGENE 6 reagent (Roche Applied Science) was used to aid transfection. Recordings were performed 29–41 h after transfection, on isolated cells expressing green fluorescent protein. The extracellular solution contained (in mM) 130 NaCl, 3.5 KCl, 1.5 MgCl₂, 3 CaCl₂, 48 NaHCO₃, 1.25 NaH₂PO₄, 10 glucose, and 1 mg/ml bovine serum albumin; pH 7.4. The 2–5 M Ω patch pipettes were filled with an intracellular solution consisting of (in mM): 135 CsCl, 2 MgCl₂, 10 HEPES, 2 Na₂-ATP, 0.2 GTP-Na₂, pH 7.2 with CsOH. Pulse and Pulsefit (HEKA) software was used for experimental protocols and analysis. Whole-cell currents were filtered at 2.9 kHz and digitized at 5 kHz. Inward currents induced by LTXs were measured and a voltage stimulation protocol (10 mV \times 40 ms steps to -90/+30 mV from holding potential of -60 mV) was applied every 1 min to check membrane conductance.

Native Electrophoresis—The recombinant toxins were subjected to native alkaline electrophoresis in 6% polyacrylamide gels as described previously (29). Prior to loading onto the gel, some samples were incubated for 5 min with 0.2% SDS (without boiling) or with 1% SDS and 5% β -mercaptoethanol (with boiling). After separation, the proteins were analyzed by immunoblotting using a polyclonal rabbit anti-LTX Ab.

Cryomicroscopy and Image Processing—Specimens for cryo-electron microscopy (cryo-EM) were prepared by applying 4- μ l aliquots of 100 μ g/ml LTX^{N4C} in TBSM onto grids containing a porous carbon foil, followed by immediate vitrification; for details and references, see Ref. 29. Images of the vitrified samples kept at -184 °C were taken in a CM200 cryomicroscope equipped with a field-emission gun, at \times 50,000 magnification and 3.1 \pm 0.1 μ m defocus. The micrographs were digitized at a step size of 14 μ m (2.8 Å on the specimen scale). Molecular images were selected interactively and processed using the IMAGIC-5 software. The images were subjected to multireference alignment and multivariate statistical classification in order to find characteristic molecular views in the sample. Symmetry of the oligomers was determined using free reference alignment followed by multistatistical analysis. Characteristic views of LTX^{N4C} were compared with re-projections of the three-dimensional maps of the LTX dimer and tetramer created using the exact filter back projection algorithm (29).

Binding Experiments—Recombinant toxins were labeled with ¹²⁵I as outlined previously (30). To study toxin dissociation from membranes, 0.5 nM iodinated LTX^{WT} or LTX^{N4C} were incubated in TBSM (plus 2 mM Ca²⁺ and 0.5 mg/ml bovine serum albumin) for 10 min, either on ice or at 37 °C, with P2 membranes (0.5 mg protein/ml) isolated from rat brain (31). The samples were then supplemented with 500 nM LTX^{NAT} (to displace the specifically bound iodinated LTXs) and transferred on ice (to prevent any further toxin incorporation into the membranes). Aliquots were taken from these reaction mixtures at specified times and filtered through GF/F filters (Whatman) to determine the remaining bound toxin. The amount of non-specifically bound LTXs was established by including 500 nM LTX^{NAT} during the initial incubation.

For binding studies, COS7 cells were transfected with LPH or NRX I α as described (9), dislodged from plates and incubated (2.5 \times 10⁵ cells/reaction) for 10 min with 1 nM [¹²⁵I]LTX^{N4C} in buffer A supplemented with EGTA, CaCl₂ or SrCl₂ as indicated in Fig. legends. Throughout this work, Sr²⁺ buffers also contained 0.2 mM EGTA to chelate any contaminating Ca²⁺, while the [SrCl₂] was adjusted to give the stated free [Sr²⁺]. Reaction mixtures were filtered through GF/F filters whose radioactivity was then measured.

The affinities of recombinant toxins for receptors in chromaffin cells were determined *in situ*, similar to catecholamine release studies (see below). After the incubation with 0–10 nM radiolabeled LTX^{WT} or LTX^{N4C} and washes, the amounts of bound toxins were established by γ -spectrometry of solubilized cells. The bound and free toxin concentrations were calculated using quantitative assessments of oligomeric states of the two toxins (determined by cryo-EM). In these experiments, the specific binding was calculated by subtracting the nonspecific binding (determined in the presence of 100-fold excess of unlabeled LTX) from the total binding.

Immunological Procedures—For immunoprecipitation experiments, the NRX Ab was purified by affinity chromatography on SH-Sepharose conjugated with the cognate peptide (NH₂-CSANKNKKNKDKEYV-COOH). P2 membranes were prepared from rat brain and liver as outlined (31). The membranes were solubilized with 1% Thesit in buffer A (1 mg of protein/ml) and divided into 200- μ l aliquots, which were incubated for 10 min with 1 nM [¹²⁵I]-LTX^{N4C} in the presence of EGTA, CaCl₂, or SrCl₂. Then, 5 μ g of the affinity-purified NRX Ab and 20 μ l of protein G-agarose (Sigma) were added to each tube and incubated for another 3 h. The radioactivity of agarose pellets was determined after two washes with buffer A containing respective additives. The immunoprecipitated proteins were eluted with the SDS-electrophoresis loading buffer, separated in 6% SDS-polyacrylamide gels, transferred onto polyvinylidene fluoride membrane (Immobilon) and visualized using the anti-NRX Ab, a peroxidase-conjugated secondary Ab and a chemiluminescent substrate (Pierce).

For detection of LTX receptors in chromaffin cells, equal samples of Triton X-100-solubilized chromaffin cells (10⁵/lane) were separated on an 8% SDS-polyacrylamide gel, transferred onto Immobilon and stained with the anti-NRX and anti-LPH Abs as above.

Biochemical Measurements of Release—Release of [¹⁴C]glutamate ([¹⁴C]Glu) was done as in Ref. 8. Briefly, synaptosomes were loaded for 5 min with [¹⁴C]Glu, washed with physiological buffer (in mM: 145 NaCl, 5 KCl, 1 MgCl₂, 10 glucose, 20 HEPES, pH 7.4), and used for release experiments 1 h later (to facilitate the labeling of both the readily releasable and depot pools of vesicles). The release was meas-

ured over 5 min after application of 0–2 nM recombinant toxins in the presence of EGTA, CaCl_2 , or SrCl_2 . In some experiments, LaCl_3 was also included in the buffer to block any toxin pores.

Bovine chromaffin cells were prepared and maintained at a density of 1×10^6 cells/well in 24-well culture plates (32). Five days later, the cells were stimulated for 15 min with 0–5 nM recombinant LTXs in buffer A containing EGTA, CaCl_2 , or SrCl_2 . Pore formation was determined simultaneously with release measurements in samples containing 2 mM CaCl_2 and 10 $\mu\text{Ci/ml}$ of $^{45}\text{Ca}^{2+}$. After the 15-min stimulation with the toxins, the media were removed; the cells were washed twice with the incubation buffer (without the radioactive tracer) and solubilized in 1% Triton X-100. The uptake of $^{45}\text{Ca}^{2+}$ was determined by scintillation counting of the solubilized cells. Catecholamine contents of the solubilized cells and media were measured fluorimetrically (32), using an automated microplate fluorimeter, Fluoroscan Ascent FL (Labsystems). Both in synaptosomes and in chromaffin cells, stimulated release was calculated by subtracting basal release in the absence of the toxins from release in their presence and expressed as a percentage of total transmitter contents.

Electrophysiological Recordings of Synaptic Transmission—Organotypic hippocampal slice cultures were prepared as described (33). Whole-cell patch-clamp recordings from CA3 pyramidal cells were performed with pipettes filled with intracellular solution (in mM, 126 K-gluconate, 10 HEPES, 10 Na_2 -phosphocreatine, 4 KCl, 4 ATP-Mg, and 0.3 GTP- Na_2 , pH 7.3). Extracellular solution (the same as in toxin channel recordings in CHO cells above) was supplemented with 1 μM tetrodotoxin, 30 μM bicuculline, 3 mM CaCl_2 , or SrCl_2 and oxygenated. The recorded neurons were voltage-clamped at -70 mV; membrane currents were amplified (10 mV/pA), low-pass filtered at 2.9 kHz, and digitized at 5 kHz. Toxin applications were done as described (34). The currents were acquired on-line using the Pulse software.

Intracellular recordings in NMJs were made using standard techniques on isolated preparations of a mouse *flexor digitorum brevis* muscle. Spontaneous miniature end-plate potentials (mepss) were recorded before and after the addition of 1 nM LTX^{N4C} . The continuously oxygenated extracellular perfusion solution (in mM: 137 NaCl, 5 KCl, 1 MgCl_2 , 5 HEPES, 5.6 glucose, 0.03 tetrodotoxin, pH 7.4) was supplemented with EGTA, Ca^{2+} , or Sr^{2+} . Recordings were made using an Axoclamp 2B amplifier (Axon Instruments); voltage signals were amplified and low-pass filtered at 3 kHz, digitized at 10 kHz using the 1401+ signal converter and recorded into Spike 4 software (Cambridge Electronic Design). The toxin was added directly to the recording chamber and thoroughly mixed with the perfusion buffer. All electrophysiological data were analyzed off-line with the MiniAnalysis software (Synaptosoft).

RESULTS

Molecular Basis of the Inability of the Mutant Toxin to Insert into Membranes and Make Pores—Both LTX^{WT} and LTX^{N4C} were expressed in baculovirus-infected insect cells (28) and affinity-purified using an immobilized mAb against LTX. A single pass through the mAb column nearly exhausted the expressed toxins from the medium and yielded essentially pure LTX^{WT} and LTX^{N4C} (Fig. 1).

We previously showed that LTX^{N4C} fails to form ionic pores in the membrane of synaptosomes and LPH-transfected BHK cells (8). Here, we confirmed and extended these observations by comparing the abilities of the recombinant toxins to induce $^{45}\text{Ca}^{2+}$ influx into COS7 cells expressing exogenous LPH or NRX. As expected, LTX^{WT} caused massive accumulation of the radioactive tracer in the cells (Fig. 2A). In contrast, LTX^{N4C} stimulated no detectable $^{45}\text{Ca}^{2+}$ influx (Fig. 2A). The lack of pore formation by even high concentrations of the mutant toxin was not due to its poor interaction with the expressed receptors because, in the same experiment, LTX^{WT} and LTX^{N4C} exhibited similar binding to both NRX- and LPH-transfected cells (Fig. 2B).

We then compared the channel-forming properties of LTX^{WT} and LTX^{N4C} by a more sensitive method, whole-cell patch-clamp recordings in CHO cells transfected with NRX or LPH. No changes in membrane conductance and no inward currents were detected after a ~ 20 min application of LTX^{N4C} (0.5, 1, and 5 nM) to cells expressing NRX or LPH (Fig. 2, C and D). In

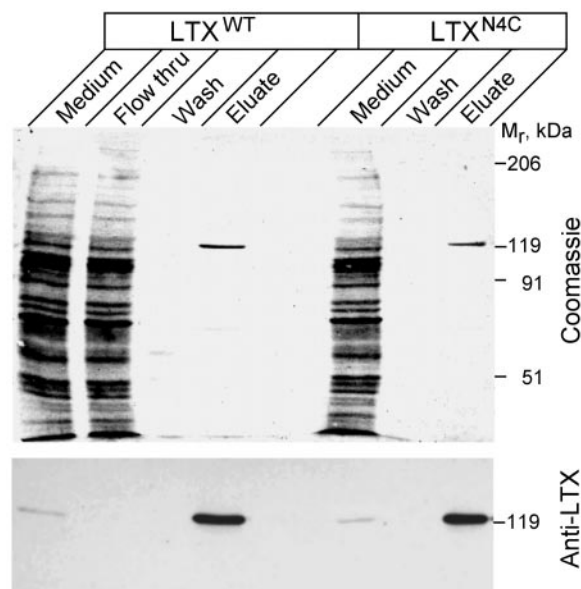


FIG. 1. Purification of LTX^{WT} and LTX^{N4C} . Recombinant toxins were purified from culture media by affinity chromatography on a mAb-Sepharose column (see “Experimental Procedures”). The starting media and chromatographic fractions were analyzed by SDS-gel electrophoresis followed by Coomassie staining (*top*) or Western blotting using the anti-LTX Ab (*bottom*). Positions of molecular mass markers are indicated on the right.

contrast, when 1 nM LTX^{WT} was subsequently applied to the same cells, a large (up to 400 pA) inward current always developed over several minutes, accompanied by an increase in membrane conductance (Fig. 2, C and D); these currents were of the same order of magnitude as those observed previously (10, 11, 35, 44), despite any differences in cell types used, transfection efficiencies, etc.

What could be the reason for such distinct behaviors of the two recombinant toxins? LTX^{N4C} differs from LTX^{WT} only by a 4-amino acid insert (Val-Pro-Arg-Gly) that has been introduced between the predicted N-terminal domain and the ankyrin repeats of LTX (Fig. 3A, *top*) in order to create a cleavage site for thrombin (17). The borderline between the domains was deduced from the toxin’s sequence. However, cryo-EM demonstrates that the domain structure of LTX is actually different (29), and that the mutation has fallen inside a tightly packed “body” domain (Fig. 3A, *middle* and *bottom*); consistently, this peptide is inaccessible to thrombin (17). Small structural changes in this region would not be expected to affect the N-terminal *wing* domain, which is presumed to participate in receptor binding (17, 29), but could perturb the overall structure of LTX and its oligomerization, which is crucial for pore formation (16, 29). To reveal any alteration of the three-dimensional structure of LTX^{N4C} induced by the insert, we used native electrophoresis, a method that had allowed us to demonstrate LTX oligomerization (29). Fig. 3B shows that, in the absence of divalent cations, both LTX^{WT} and LTX^{N4C} normally existed as dimers, although LTX^{N4C} had a slightly lower mobility, which was probably due to its partial unfolding caused by the insert. The addition of 0.2% SDS, known to induce oligomerization of LTX during native electrophoresis (29), clearly produced several bands in the LTX^{WT} sample that corresponded to monomers, dimers, and tetramers. However, the tetramers were absent from the equally treated LTX^{N4C} (Fig. 3B), suggesting that it was easily denatured by 0.2% SDS and lost an ability to assemble into higher oligomers. Upon boiling in 1% SDS, both toxins became monomeric and, as expected, displayed the same electrophoretic mobility.

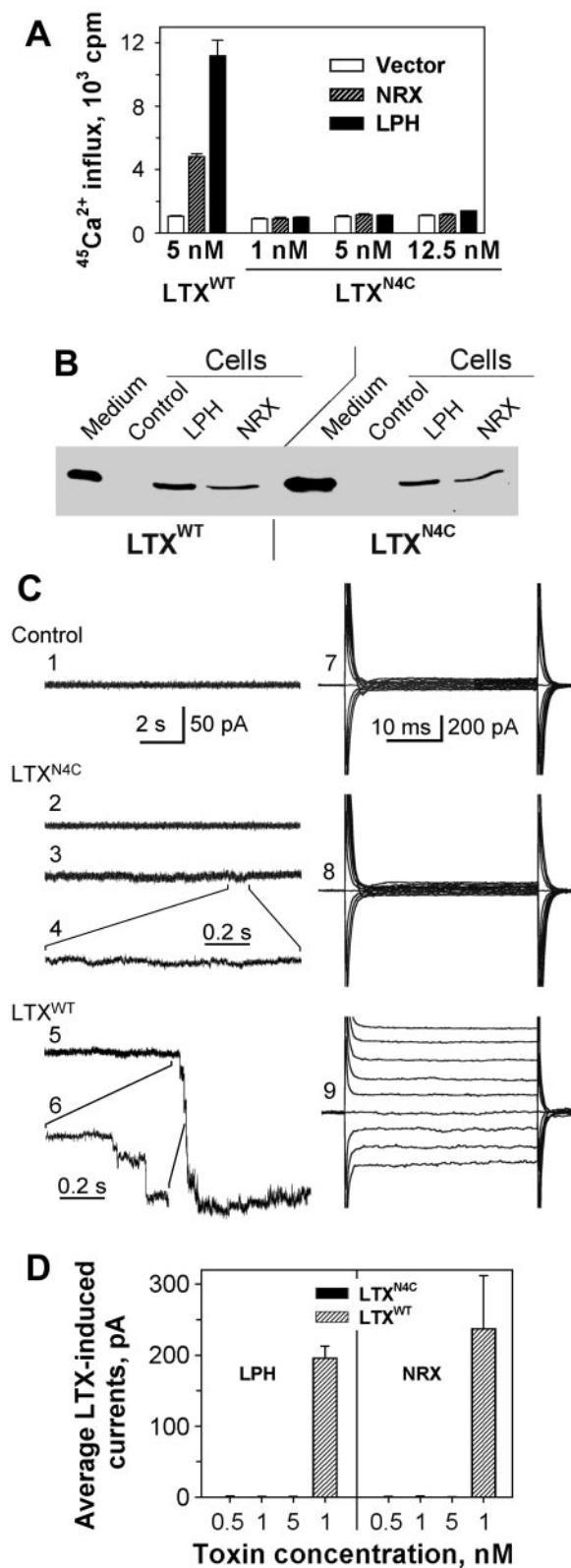


FIG. 2. LTX^{N4C} is unable to form ionic pores. *A*, influx of $^{45}\text{Ca}^{2+}$ induced by recombinant LTXs (measured as described under "Experimental Procedures"). The data are the means \pm S.E. from a typical experiment done in triplicates. *B*, both recombinant toxins bind to COS7 cells expressing LPH or NRX. The cells from *A* (incubated with 5 nM recombinant toxins) were harvested and analyzed by Western blotting, using the anti-LTX Ab. *C* and *D*, LTX^{WT} , but not LTX^{N4C} , induces inward currents in receptor-transfected CHO cells. *C*, whole-cell patch-clamp traces 1–9 were recorded in the presence of 3 mM Ca^{2+} 36 h after transfection with LPH. Recordings at -60 mV were done before (trace 1) and after the addition of 1 nM LTX^{N4C} (traces 2–4). LTX^{N4C} caused no

The nature of LTX^{N4C} oligomers was then studied by cryo-EM, which allows the observation of molecules that have been instantaneously frozen in their physiological states. The characteristic molecular images of LTX^{N4C} were similar in size and shape to re-projections of the three-dimensional model of the LTX^{NAT} dimer (Fig. 3C) (29), indicating that the mutant was indeed dimeric. However, the LTX^{N4C} dimers were slightly more flexible and displayed some deviations from the structure of similarly oriented wild-type dimers (e.g. classes III and V in Fig. 3C). Much more striking was the fact that the tetramers, which under the conditions of this experiment constitute $96 \pm 3\%$ of identifiable wild-type toxin particles (Fig. 3C, class VI) (16, 29) have never been observed in LTX^{N4C} samples.

It has been postulated that LTX must assemble into cyclical tetramers in order to insert itself into membranes and form pores (16, 29), and our results implied that because the mutant toxin did not make tetramers, it should be incapable of membrane insertion. To support this idea, we demonstrated that the dissociation of LTX^{N4C} from receptor-containing membranes did not depend on the incubation temperature during binding and always followed the same first order kinetics (Fig. 3D). This experiment could only be explained by the inability of the mutant to insert into membranes at any temperature. In total contrast, the dissociation of the wild-type LTX was greatly affected by the temperature during binding (Fig. 3D): if the binding was carried out at 37°C , only $\sim 25\%$ of LTX^{WT} could dissociate afterward, whereas about 75% never dissociated due to permanent incorporation into the membrane. As expected, at 0°C , the behavior of LTX^{WT} was intermediate, consistent with restricted incorporation into the membrane at low temperatures (Fig. 3D).

Thus, our combined data not only ascertain the lack of pore formation by the mutant toxin, but also explain this feature at the molecular level. These findings further indicate that LTX^{N4C} can cause exocytosis only by a reversible interaction with its receptors. Experiments below were designed to answer the question of the relative importance of the two LTX receptors, LPH and NRX, for the receptor-mediated action of the mutant toxin.

NRXs Do Not Bind LTX^{N4C} in the Presence of Sr^{2+} —We showed previously that Sr^{2+} could fully replace Ca^{2+} in supporting LTX-evoked release of [^3H]norepinephrine from rat synaptosomes (5). At the same time, no interaction between NRX I α and LTX could be detected in the presence of Sr^{2+} . However, in the current work we used a recombinant, mutant toxin, so it was necessary to ascertain that it had the same divalent cation requirement for binding as native LTX. To test this, we transiently expressed LPH or NRX I α in COS7 cells,

inward current during the time of recording (5–20 min; trace 2), although in 2 of 6 cells small current fluctuations were observed (trace 3); these were rare and transient and did not represent the toxin pore as demonstrated by expanded trace 4 (compare with trace 6 below). In contrast, when 1 nM LTX^{WT} was subsequently applied, in less than 2 min an inward current of ~ 200 pA (trace 5) appeared that continued to the end of recording. The stepwise opening of first LTX^{WT} pores is shown by expanded trace 6. During these recordings, voltage steps (10 mV, 40 ms) were applied every 1 min before (trace 7) and after (traces 8, 9) toxin additions. Only LTX^{WT} (trace 9), but not LTX^{N4C} (trace 8), enhanced currents evoked by voltage steps, indicating that only LTX^{WT} caused an increase in membrane conductance. Scale bars at the top apply to traces 1–6 and 7–9, respectively, except an expanded time scale applies to traces 4 and 6. *D*, average currents evoked by LTX^{WT} and LTX^{N4C} in CHO cells transfected with LPH or NRX. Currents were averaged over several random 10 s intervals 5 min after toxin additions, and the data are the means \pm S.E. of three experiments for each receptor. In the presence of 0.5–5 nM LTX^{N4C} , the average currents did not differ from the background, whereas in the presence of 1 nM LTX^{WT} , continuous inward currents fluctuated near 196 ± 17 and 237 ± 75 pA in cells transfected with LPH and NRX, respectively.

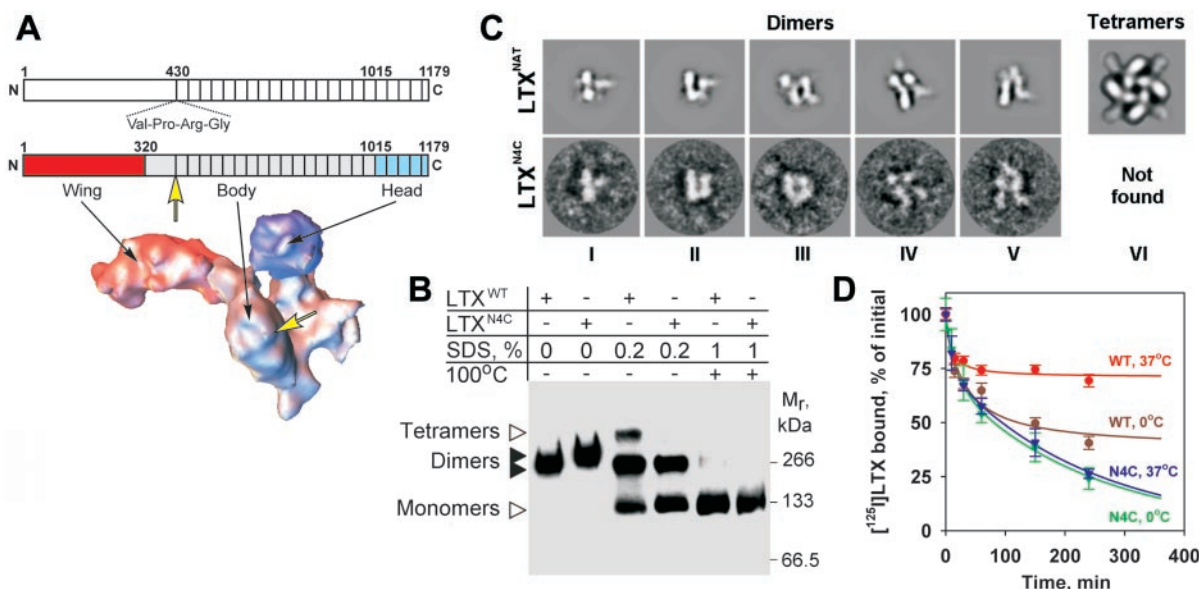


FIG. 3. Molecular evidence for the inability of LTX^{N4C} to insert into membranes and form pores. *A*, *top*, schematic representation of the domain structure of LTX based on sequence analysis. The position and sequence of the LTX^{N4C} insert is shown *below*; *small boxes* represent ankyrin repeats. *Middle*, the domain structure of LTX re-evaluated using the cryo-EM data (29). The position of the insert is shown by an *arrow*; the colors denote: *red*, the N-terminal *wing* domain; *gray*, the central *body* domain; *blue*, the C-terminal *head* domain. *Bottom*, The three-dimensional structure of the LTX monomer. The domains are colored as above; the *arrow* indicates an approximate position of the insert. *B*, in the absence of divalent cations, both LTX^{WT} and LTX^{N4C} are dimeric. 0.2% SDS induces the oligomerization of LTX^{WT} but not LTX^{N4C}. The purified toxins (untreated or treated, as indicated) were directly loaded into the wells of non-denaturing polyacrylamide gels, separated, and Western blotted as described under “Experimental Procedures.” The results are representative of six experiments. *C*, only LTX^{WT}, but not LTX^{N4C}, is able to form tetramers. Cryo-EM of the native and mutant toxins was carried out as outlined under “Experimental Procedures.” The characteristic molecular images of LTX^{N4C} (*bottom row*, consisting of the following numbers of individual images: *I*, 211; *II*, 303; *III*, 374; *IV*, 175; *V*, 273) are aligned with similar re-projections of the three-dimensional model of LTX^{NAT} (*top row*). The datasets contained ~5,000 and ~3,000 individual molecular images for LTX^{NAT} and LTX^{N4C}, respectively. *D*, dissociation of LTX^{WT} and LTX^{N4C} from brain membranes. The membranes were incubated with the iodinated recombinant LTXs at 0 °C or 37 °C; the rates of toxin dissociation were measured as described under “Experimental Procedures.” The data are the means \pm S.E. from a typical experiment done in triplicates. Note that LTX^{WT}, but not LTX^{N4C}, can permanently incorporate into the membranes.

which do not contain endogenous LPH or NRXs. As expected, LPH-expressing cells bound ¹²⁵I-LTX^{N4C} under all conditions tested, while NRX-expressing cells were able to bind the mutant toxin only in the presence of Ca²⁺ (Fig. 4A).

This result was based on the use of NRX α and could not be automatically extended to neurons, which additionally contain other members of the NRX family that have slightly different ionic requirements for LTX binding (22). An experiment was then designed to detect LTX^{N4C} binding to any NRX variant. For this purpose, solubilized rat brain membranes were mixed with ¹²⁵I-LTX^{N4C} in the presence of EGTA, Ca²⁺, or Sr²⁺ and then immunoprecipitated using an antibody that equally recognizes the C termini of all NRXs. As a control of specificity, we used rat liver membranes that lack NRXs (18). Fig. 4B (*upper panel*) demonstrates that independently of the ionic conditions used, this procedure brought down both the α - and β - forms of NRXs from brain. However, ¹²⁵I-LTX^{N4C} co-immunoprecipitated with NRXs specifically only in the medium containing Ca²⁺ (Fig. 4B, *lower panel*), while neither EGTA nor Sr²⁺ supported any interaction between the mutant toxin and NRXs.

These results demonstrate unequivocally that, similar to native toxin, the mutant LTX^{N4C} binds to all NRXs in a strictly Ca²⁺-dependent manner and that Sr²⁺ cannot sustain this interaction. Using this approach, we then asked whether the involvement of NRXs was critical for LTX^{N4C}-stimulated release of neurotransmitters in several model systems based on either biochemical or electrophysiological detection of exocytosis.

LTX^{N4C}-evoked Release of [¹⁴C]Glu from Rat Synaptosomes—As mentioned above, LTX^{N4C} stimulates receptor-mediated exocytosis of amino acid neurotransmitters from synap-

tosomes only in the presence of Ca²⁺ (8). In the current work, we substituted Ca²⁺ with Sr²⁺. Synaptosomes were loaded with [¹⁴C]Glu and stimulated by different concentrations of LTX^{N4C} in a buffer containing EGTA, Ca²⁺ or Sr²⁺. As expected, the mutant toxin was inactive in the presence of EGTA (*i.e.* when the only divalent cation present was Mg²⁺), but capably stimulated [¹⁴C]Glu release in the Ca²⁺-containing buffer (Fig. 5A). Interestingly, in the presence of Sr²⁺, LTX^{N4C} was also able to trigger exocytosis, and the amount of this release was not statistically different from that in Ca²⁺-containing medium (Fig. 5A).

Did LTX^{N4C} require Ca²⁺ or Sr²⁺ simply because it produced a small number of pores that allowed these cations to enter nerve terminals and evoke secretion? Although we have demonstrated above that the mutant toxin cannot form pores and also showed previously that LTX^{N4C} did not allow influx of ⁴⁵Ca²⁺ into synaptosomes (8), it was still necessary to prove that in our release experiments the mutant toxin acted only via receptor stimulation. To distinguish between the receptor- and pore-mediated actions, we used La³⁺ known to efficiently block LTX pores (8, 35). The idea was that if the mutant's effect had been even partially based on pore formation, it should be inhibited by La³⁺. Indeed, this cation strongly attenuated Glu release (Fig. 5B) caused by LTX^{WT}, which acts via both receptor and pores. In particular, the Ca²⁺-independent release was abolished, while the Ca²⁺- and Sr²⁺-dependent secretion was brought to the levels normally evoked by LTX^{N4C} (see also “Discussion”). In contrast, transmitter secretion stimulated by LTX^{N4C} in the presence of either Ca²⁺ or Sr²⁺ was not at all affected by La³⁺ (Fig. 5B). This ability of the pore-blocking cation to partially inhibit the action of the wild type but not the

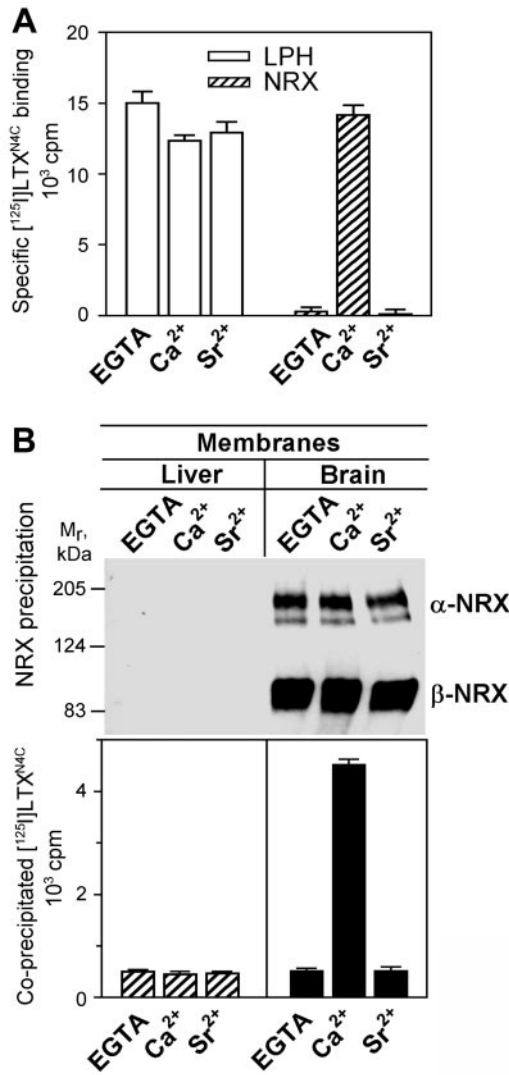


FIG. 4. Sr²⁺ does not sustain interaction between LTX^{N4C} and NRXs. *A*, specific binding of [¹²⁵I]-LTX^{N4C} to COS7 cells expressing LPH or NRX α , in the presence of 0.2 mM EGTA, 2 mM CaCl₂, or 2 mM SrCl₂. *B*, co-immunoprecipitation of [¹²⁵I]-LTX^{N4C} with α - and β -NRXs from solubilized rat brain membranes using anti-NRX C-terminal antibody, in the presence of 0.2 mM EGTA, 2 mM CaCl₂, or 2 mM SrCl₂. The precipitated samples were analyzed by Western blotting (*upper panel*) and γ -spectrometry (*lower panel*) as described under "Experimental Procedures." Liver membranes were used to control the specificity of precipitation. The data are from representative experiments done in triplicates and where applicable represents the means \pm S.E. Note that the mutant toxin interacts specifically with NRXs in the presence of Ca²⁺ but not Sr²⁺.

mutant LTX did not depend on the concentration of toxins used (data not shown).

Thus, pore formation does not play any detectable role in the Ca²⁺/Sr²⁺-dependent Glu release triggered by LTX^{N4C} in synaptosomes, and this secretion can occur without the participation of NRXs.

Secretion of Catecholamines from Bovine Chromaffin Cells—LTX is known to efficiently stimulate exocytosis of LDCV containing catecholamines and hormones in chromaffin and PC12 cells; this action is strictly Ca²⁺-dependent (6, 36).

First, we ascertained that bovine chromaffin cells expressed endogenous LPH and NRX. Toxin binding to these cells was higher in Ca²⁺-containing buffers than in EGTA (Fig. 6A, *upper panel*), indicating the presence of Ca²⁺-dependent receptors, which corresponded to NRXs, as demonstrated by Western blotting (Fig. 6A, *lower panel*). Immunostaining also

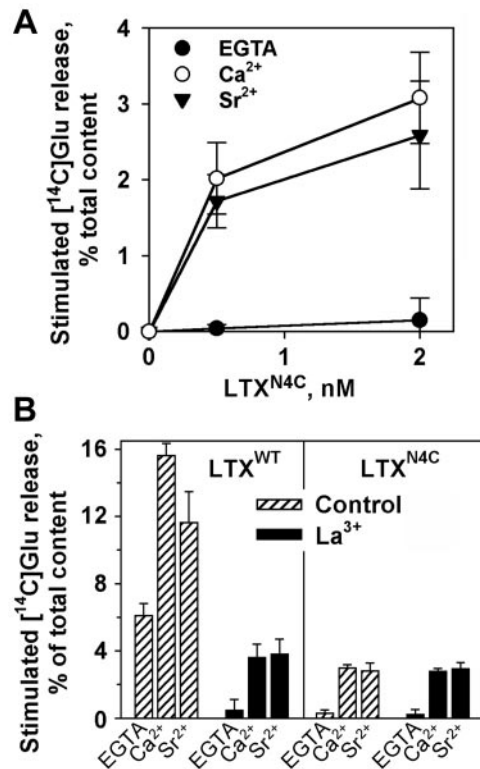


FIG. 5. Sr²⁺ supports [¹⁴C]Glu release stimulated by the mutant toxin in synaptosomes. *A*, dose dependence of LTX^{N4C}-evoked release of [¹⁴C]Glu from rat synaptosomes in the presence of 0.1 mM EGTA, 1.2 mM Ca²⁺ or 1.2 mM Sr²⁺. *B*, the effect of 0.1 mM La³⁺ on [¹⁴C]Glu release triggered by 1 nM LTX^{WT} or LTX^{N4C} under the ionic conditions described in *A*. In both experiments, secretion was measured as outlined under "Experimental Procedures." The data are the means \pm S.E. from two independent experiments done in triplicates. Note that Ca²⁺ and Sr²⁺ equally support Glu exocytosis induced by mutant toxin and that La³⁺ does not affect the LTX^{N4C}-evoked release but strongly inhibits the action of LTX^{WT}.

showed that the Ca²⁺-independent receptors were represented by LPH.

We then compared LTX^{N4C} with wild type toxin in terms of binding to chromaffin cells *in situ*. As demonstrated in Fig. 6B, the dissociation constants and the numbers of binding sites were equal for both toxins (0.26 nM and 5.2 fmol/10⁶ cells, respectively).

LTX^{WT} and LTX^{N4C} were then used to stimulate release of endogenous catecholamines and influx of Ca²⁺ into chromaffin cells. Despite similar binding of the two toxins to these cells, LTX^{WT} caused a stronger transmitter secretion than did LTX^{N4C} by acting via both receptor- and pore-dependent mechanisms (Fig. 6C). Consistently, release stimulated by the wild-type toxin was associated with massive influx of ⁴⁵Ca²⁺ (Fig. 6D). In agreement with the previously published data (6, 22), the bell-shaped secretion curve indicated that catecholamine release was mainly stimulated by Ca²⁺ entry via toxin pores. Indeed, while exocytosis correlated with intracellular [Ca²⁺] at lower [LTX^{WT}], excessive Ca²⁺ influx induced by 3–5 nM LTX^{WT} inhibited release as in Ref. 6. Note that the apparent decrease in ⁴⁵Ca²⁺ uptake at the highest LTX^{WT} concentration was not caused by inhibition of LTX pores but rather by disproportionately easy escape of Ca²⁺ through multiple toxin pores during extensive washing; this effect was less evident at lower toxin doses. In contrast to LTX^{WT}, the mutant did not cause any detectable uptake of ⁴⁵Ca²⁺ (Fig. 6D), confirming that it does not form pores but acts via the receptor-mediated mechanism. Finally, we tested the effect of mutant toxin on

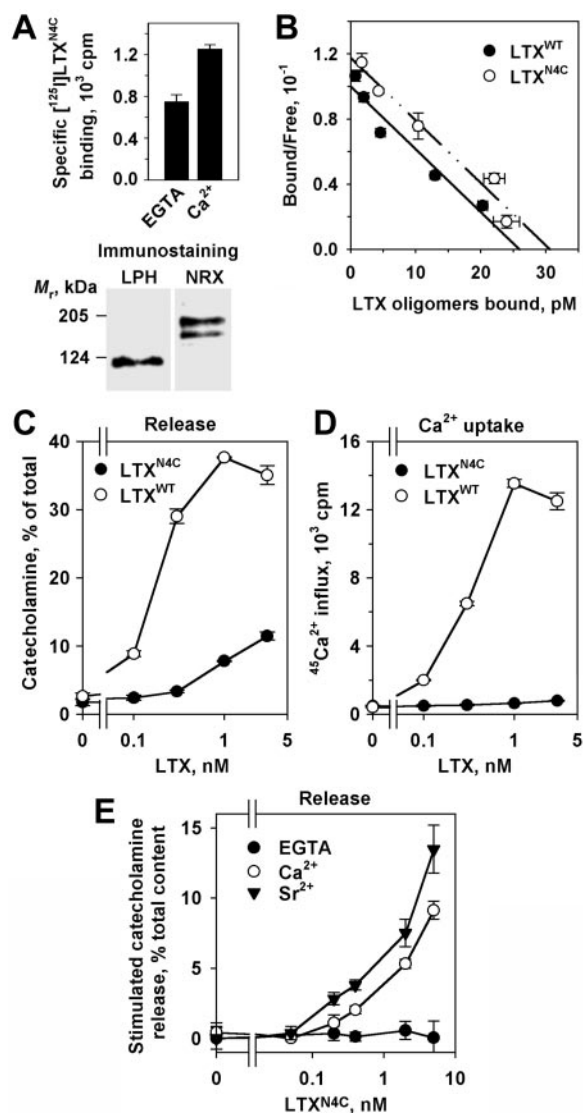


FIG. 6. Sr^{2+} supports LTX^{N4C} -stimulated catecholamine release from bovine chromaffin cells. *A*, LTX receptors in chromaffin cells. *Upper panel*, binding of [^{125}I] LTX^{N4C} to the cells in the presence of 0.2 mM EGTA or 2.2 mM Ca^{2+} (1 nM [^{125}I] LTX^{N4C} was used). *Lower panel*, immunodetection of NRX and LPH in chromaffin cells. *B*, LTX^{N4C} and LTX^{WT} have the same affinities for the receptors and the same number of binding sites in chromaffin cells. The experiment was carried out in the presence of 2.2 mM Ca^{2+} . *C* and *D*, release of endogenous catecholamines and uptake of $^{45}\text{Ca}^{2+}$ induced by LTX^{WT} and LTX^{N4C} in chromaffin cells. The cells were stimulated by different concentrations of the recombinant toxins in the presence of 2.2 mM Ca^{2+} and 10 $\mu\text{Ci/ml}$ of $^{45}\text{Ca}^{2+}$. *E*, effects of LTX^{N4C} on secretion of catecholamines from chromaffin cells in the presence of 0.2 mM EGTA, 2.2 mM Ca^{2+} , or 2.2 mM Sr^{2+} . For details of toxin binding, catecholamine release, Ca^{2+} influx and immunological procedures, see "Experimental Procedures." The data in the figure are the means \pm S.E. from representative experiments done in triplicates. Note that (i) the wild-type toxin, but not the mutant, stimulates massive $^{45}\text{Ca}^{2+}$ influx, and (ii) Sr^{2+} efficiently supports the LTX^{N4C} -stimulated release.

transmitter exocytosis in the presence of either Ca^{2+} or Sr^{2+} . Again, LTX^{N4C} was as efficient in Sr^{2+} as it was in Ca^{2+} (Fig. 6E).

LTX^{N4C} -induced Spontaneous Release of Glu in Rat Hippocampal Cultures—Recently, we showed that LTX^{N4C} dramatically increases the frequency of Glu-mediated miniature excitatory post-synaptic currents (mEPSCs) in hippocampal slices (8). In this system too, the mutant toxin is active only in the presence of calcium (45). In the current study, we compared the effects of LTX^{N4C} in the presence of Ca^{2+} and Sr^{2+} . The

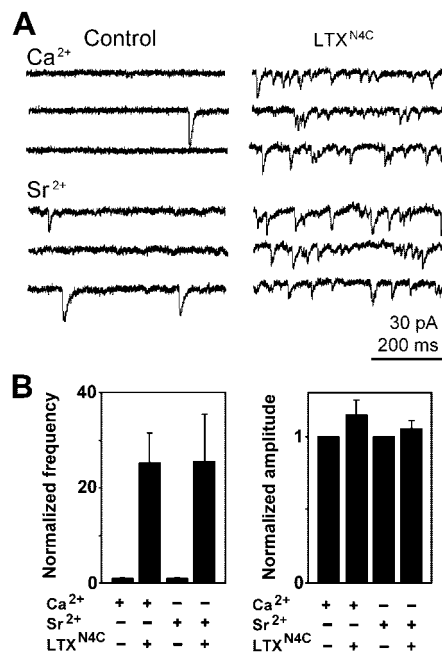


FIG. 7. Both Ca^{2+} and Sr^{2+} support the LTX^{N4C} -evoked increase in mEPSCs frequency in hippocampal slices. *A*, representative recordings of mEPSCs before (*Control*) and after application of 1 nM LTX^{N4C} . The basal mEPSCs frequencies were 0.6 Hz in 3 mM CaCl_2 and 1.5 Hz in 3 mM SrCl_2 . These increased, respectively, to 20.9 Hz and 23.7 Hz in the presence of mutant toxin. *B*, Mean mEPSCs frequencies and amplitudes (\pm S.E.) normalized to control value for each cell ($n = 4$ for each condition). Note that LTX^{N4C} increases mEPSCs frequency to a similar extent in the presence of Ca^{2+} or Sr^{2+} and has no effect on the mean mEPSCs amplitudes.

results shown in Fig. 7 demonstrate that LTX^{N4C} increased the mEPSCs frequency in Sr^{2+} -containing buffer approximately to the same extent as in the presence of Ca^{2+} (25-fold on average). At the same time, LTX^{N4C} had no effect on the mean mEPSCs amplitude under any condition, indicating that the mutant acted presynaptically in both media (Fig. 7B).

LTX^{N4C} -evoked Spontaneous Exocytosis of Acetylcholine at Mouse NMJs—Although LTX effect of at the NMJ has been extensively studied (37–40) it remains largely unexplained due to the multiple actions of native toxin (1, 40). Therefore, the use of LTX^{N4C} , which fails to form pores or penetrate into the cytosol, should greatly simplify the interpretation of results.

When tested on mouse NMJs, the mutant toxin consistently exhibited the same effects as in the other systems: it was inactive in the presence of EGTA over the period of hours² but caused a profound increase in mepps frequency when the medium was supplemented with Ca^{2+} or Sr^{2+} (Fig. 8A). Normalized data from 11 muscle fibers (Fig. 8B) indicate that the mutant toxin caused a similar (~ 70 -fold) increase in the mepps frequency in the presence of these divalent cations. As in hippocampal cultures, the amplitude of the miniature events remained the same under all conditions, demonstrating the presynaptic site of LTX^{N4C} action (Fig. 8B).

DISCUSSION

The mechanism of action of the wild-type (or native) LTX consists of receptor binding/stimulation and pore formation, making it difficult to reveal the individual roles of the two major high affinity LTX receptors, NRX I α and LPH (2). Although these structurally unrelated receptors are unlikely to

² A detailed study of the role of Ca^{2+} in the LTX^{N4C} action at the NMJ will be published elsewhere (K. E. Volynski, D. Thomson, R. R. Ribchester, and Y. A. Ushkaryov, paper in preparation).

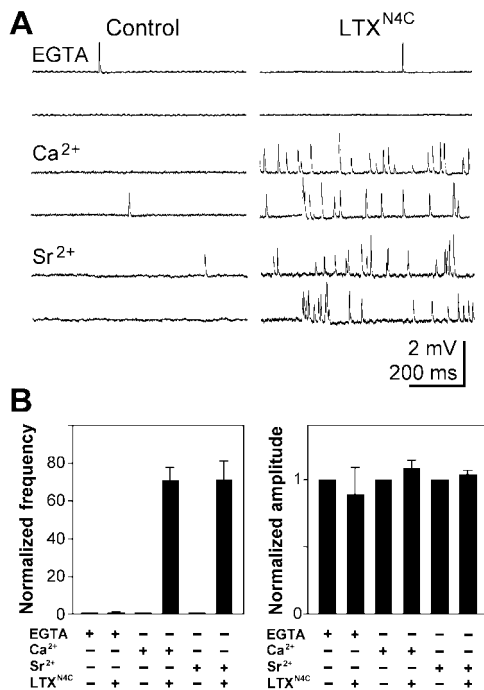


FIG. 8. LTX^{N4C} increases the rate of mepps at mouse NMJs in the presence of either Ca²⁺ or Sr²⁺. *A*, representative recordings of mepps before (*Control*) and after application of 1 nM LTX^{N4C} in the presence of 5 mM EGTA, 2 mM CaCl₂, or 2 mM SrCl₂. On average, the frequency of mepps was 0.13 ± 0.05 Hz at rest (not statistically different in the presence of EGTA, Ca²⁺, or Sr²⁺). After the addition of LTX^{N4C}, the frequency remained at 0.13 ± 0.02 Hz ($n = 3$) in 5 mM EGTA but rose to 9.12 ± 0.9 ($n = 4$) or 10 ± 1.4 ($n = 4$) in 2 mM Ca²⁺ or Sr²⁺, respectively. *B*, mean mepps frequencies and amplitudes (±S.E.) normalized to control value for each fiber ($n = 3$ for EGTA and 4 for Ca²⁺ and Sr²⁺). Note that LTX^{N4C} is inactive in EGTA but dramatically raises the mepps frequency in the presence of Ca²⁺ or Sr²⁺ and has no effect on the mepps amplitude.

couple to one signaling system, they both can efficiently support the pore-forming activity of LTX^{WT} by recruiting toxin tetramers to the cell surface and facilitating their incorporation into the membrane (9, 29). This explains why NRXs, LPH, or even their signal-deficient mutants, over-expressed in chromaffin and PC12 cells, sensitize these cells to native/wild type LTX (22, 41): all receptors increase the number of toxin pores in the cell membrane (9–11, 41). Receptor gene knockout has also given unclear results (42, 43) because the pore-forming LTX^{WT} remained active even in mice lacking either of these receptors; however, the simultaneous knockout of both receptors dramatically reduced toxin activity (43). Possible interaction of LPH and NRX I α (2) and the ability of LTX to bind many NRX variants (22) hinder this approach even further and necessitate a simultaneous knockout of all NRXs.

Therefore, the system had to be simplified. First, it was necessary to prevent all the activities of LTX^{WT} associated with its incorporation into the membrane and resulting in pore formation and/or interaction with intracellular proteins. For this purpose, we used the mutant LTX^{N4C}, which, as we have demonstrated (Figs. 2 and 3) (8), is unable to insert into the membrane and form pores but can only act via receptor stimulation. Second, we needed to exclude the toxin's interaction with one receptor type. NRXs were chosen for two reasons: (i) they were apparent candidates to mediate the receptor-transduced LTX action, which critically required Ca²⁺ (5, 8), and (ii) toxin binding to all members of the NRX family could be totally abolished by a simple replacement of Ca²⁺ with Sr²⁺ (5) (Fig. 4). This eliminated the need for multiple gene knockouts. Im-

portantly, the use of Sr²⁺ did not alter the interaction of LTX^{N4C} with LPH (Fig. 4A).

With this approach, we have found that Sr²⁺ could fully substitute Ca²⁺ in LTX^{N4C}-evoked exocytosis of Glu-containing SVs in rat synaptosomes (Fig. 5A) and hippocampal cultures (Fig. 7), acetylcholine-containing SVs at mouse NMJs (Fig. 8), and catecholamine-containing LDCVs in bovine chromaffin cells (Fig. 6E). In all the models, the mutant toxin was inactive when only Mg²⁺ was present, confirming our previous observation that receptor-mediated LTX-evoked secretion requires extracellular Ca²⁺ (5, 8).

The dependence of the LTX^{N4C} effect on the presence of Ca²⁺ or Sr²⁺, both of which can stimulate exocytosis upon entering the cytosol, could potentially mean that the mutant toxin simply acted as an ionophore, if only less potent than LTX^{WT}. However, we show that LTX^{N4C} does not form cation-permeable pores in synaptosomes (8), hippocampal slice cultures², chromaffin cells (Fig. 6D), and different types of receptor-transfected cells (8) (Fig. 2, A and C). Our present results further indicate that the pore-forming ability is the main distinction between LTX^{N4C} and LTX^{WT}. Indeed, although LTX^{WT} stimulates a stronger secretion than does LTX^{N4C}, this difference (i) is abolished by La³⁺, which blocks LTX pores (in synaptosomes); and (ii) correlates with Ca²⁺ influx (in chromaffin cells). In contrast, the effect of LTX^{N4C} is insensitive to La³⁺ (Fig. 5B) and does not associate with Ca²⁺ entry (8) (Fig. 6D).

Our experiments also provide a molecular explanation of the inability of the mutant LTX to form pores. LTX^{WT} induces pores by assembling into cyclical tetramers that possess a central channel and a hydrophobic base, which allows the toxin to incorporate into the membrane (29). We demonstrate here that LTX^{N4C} cannot make tetramers; as a result, it lacks the exposed hydrophobic domain and must be unable to insert into membranes. Indeed, the mutant toxin readily dissociates from brain membranes, whereas LTX^{WT} becomes permanently incorporated into the membrane in a temperature-dependent manner (Fig. 3D). These findings are consistent with the data on protease protection (12), which also suggested that the mutant was incapable of membrane insertion.

Our results, thus, indicate that LTX^{N4C}-evoked release is mediated by receptors. In addition, the amount of secretion induced by LTX^{N4C} in all the systems is similar regardless of NRX participation in toxin binding. Thus, although we cannot totally rule out some involvement of NRX I α in LTX signaling, NRX is not critical for the receptor-mediated release.

Taken together, these findings strongly implicate LPH as the main LTX receptor that transduces an exocytotic signal. This signaling is masked by massive Ca²⁺ influx leading to exocytosis when LTX^{WT} is used and can only be clearly demonstrated with LTX^{N4C}. It is currently unclear why the mutant toxin binds LPH under all conditions but requires extracellular Ca²⁺ or Sr²⁺ to induce exocytosis. It is possible that these divalent cations (i) serve as extracellular co-factors for LPH and its signaling partners, (ii) participate in the activation of intracellular Ca²⁺ stores required for LTX^{N4C}-induced release (45) or (iii) directly induce secretion after entering the cell via some LPH-linked cation channels. The latter hypothesis is interesting but at present seems implausible because these hypothetical channels are undetectable electrophysiologically or biochemically and must be very unusual, being insensitive to La³⁺, Cd²⁺, SKF 96365 and other drugs (45). Future research will concentrate on the mechanisms of the LPH-transduced LTX action and the roles of Ca²⁺ and Sr²⁺ in this process.

Acknowledgments—We thank E. Grishin for the help with expression of recombinant toxins and for providing the anti-LTX mAb and to G. O'Sullivan for help with isolation and maintenance of chromaffin cells.

REFERENCES

1. Rosenthal, L., and Meldolesi, J. (1989) *Pharmacol. Ther.* **42**, 115–134
2. Südhof, T. C. (2001) *Annu. Rev. Neurosci.* **24**, 933–962
3. Ushkaryov, Y. (2002) *Toxicol.* **40**, 1–5
4. Meldolesi, J. (1982) *J. Neurochem.* **38**, 1559–1569
5. Davletov, B. A., Meunier, F. A., Ashton, A. C., Matsushita, H., Hirst, W. D., Lelianova, V. G., Wilkin, G. P., Dolly, J. O., and Ushkaryov, Y. A. (1998) *EMBO J.* **17**, 3909–3920
6. Bittner, M. A., Krasnoperov, V. G., Stuenkel, E. L., Petrenko, A. G., and Holz, R. W. (1998) *J. Neurosci.* **18**, 2914–2922
7. Bittner, M. A., and Holz, R. W. (2000) *J. Biol. Chem.* **275**, 25351–25357
8. Ashton, A. C., Volynski, K. E., Lelianova, V. G., Orlova, E. V., Van Renterghem, C., Canepari, M., Seagar, M., and Ushkaryov, Y. A. (2001) *J. Biol. Chem.* **276**, 44695–44703
9. Volynski, K. V., Meunier, F. A., Lelianova, V. G., Dudina, E. E., Volkova, T. M., Rahman, M. A., Manser, C., Grishin, E. V., Dolly, J. O., Ashley, R. H., and Ushkaryov, Y. A. (2000) *J. Biol. Chem.* **275**, 41175–41183
10. Hlubek, M. D., Stuenkel, E. L., Krasnoperov, V. G., Petrenko, A. G., and Holz, R. W. (2000) *Mol. Pharmacol.* **57**, 519–528
11. Van Renterghem, C., Iborra, C., Martin-Moutot, N., Lelianova, V., Ushkaryov, Y., and Seagar, M. (2000) *Eur. J. Neurosci.* **12**, 3953–3962
12. Khvotchev, M., and Südhof, T. C. (2000) *EMBO J.* **19**, 3250–3262
13. Queiroz, L. S., and Duchen, L. W. (1982) *Proc. R. Soc. Lond. B. Biol. Sci.* **216**, 103–110
14. Watanabe, O., Torda, M., and Meldolesi, J. (1983) *Neuroscience* **10**, 1011–1024
15. Mallart, A., and Haimann, C. (1985) *Muscle Nerve* **8**, 151–157
16. Ashton, A. C., Rahman, M. A., Volynski, K. E., Manser, C., Orlova, E. V., Matsushita, H., Davletov, B. A., van Heel, M., Grishin, E. V., and Ushkaryov, Y. A. (2000) *Biochimie. (Paris)* **82**, 453–468
17. Ichtchenko, K., Khvotchev, M., Kiyatkin, N., Simpson, L., Sugita, S., and Südhof, T. C. (1998) *EMBO J.* **17**, 6188–6199
18. Ushkaryov, Y. A., Petrenko, A. G., Geppert, M., and Südhof, T. C. (1992) *Science* **257**, 50–56
19. Lelianova, V. G., Davletov, B. A., Sterling, A., Rahman, M. A., Grishin, E. V., Totty, N. F., and Ushkaryov, Y. A. (1997) *J. Biol. Chem.* **272**, 21504–21508
20. Krasnoperov, V. G., Bittner, M. A., Beavis, R., Kuang, Y., Salnikow, K. V., Chepurny, O. G., Little, A. R., Plotnikov, A. N., Wu, D., Holz, R. W., and Petrenko, A. G. (1997) *Neuron* **18**, 925–937
21. Ushkaryov, Y. A., and Südhof, T. C. (1993) *Proc. Natl. Acad. Sci. U. S. A.* **90**, 6410–6414
22. Sugita, S., Khvotchev, M., and Südhof, T. C. (1999) *Neuron* **22**, 489–496
23. Davletov, B. A., Krasnoperov, V., Hata, Y., Petrenko, A. G., and Südhof, T. C. (1995) *J. Biol. Chem.* **270**, 23903–23905
24. Ichtchenko, K., Bittner, M. A., Krasnoperov, V., Little, A. R., Chepurny, O., Holz, R. W., and Petrenko, A. G. (1999) *J. Biol. Chem.* **274**, 5491–5498
25. Matsushita, H., Lelianova, V. G., and Ushkaryov, Y. A. (1999) *FEBS Lett.* **443**, 348–352
26. Lang, J., Ushkaryov, Y., Grasso, A., and Wollheim, C. B. (1998) *EMBO J.* **17**, 648–657
27. Rahman, M. A., Ashton, A. C., Meunier, F. A., Davletov, B. A., Dolly, J. O., and Ushkaryov, Y. A. (1999) *Phil. Trans. R. Soc. Lond. B.* **354**, 379–386
28. Volynski, K. E., Nosyreva, E. D., Ushkaryov, Y. A., and Grishin, E. V. (1999) *FEBS Lett.* **442**, 25–28
29. Orlova, E. V., Rahman, M. A., Gowen, B., Volynski, K. E., Ashton, A. C., Manser, C., van Heel, M., and Ushkaryov, Y. A. (2000) *Nat. Struct. Biol.* **7**, 48–53
30. Ushkarev, Iu. A., and Grishin, E. V. (1986) *Bioorg. Khim.* **12**, 71–80
31. Phelan, P., and Gordon-Weeks, P. R. (1997) in *Neurochemistry. A Practical Approach* (Turner, A. J., and Bachelard, H. S., eds) pp. 1–38, IRL Press, Oxford
32. Lawrence, G. W., Weller, U., and Dolly, J. O. (1994) *Eur. J. Biochem.* **222**, 325–333
33. Stoppini, L., Buchs, P. A., and Muller, D. (1991) *J. Neurosci. Methods* **37**, 173–182
34. Capogna, M., Gähwiler, B. H., and Thompson, S. M. (1996) *J. Neurophysiol.* **76**, 3149–3158
35. Hurlbut, W. P., Chierregatti, E., Valtorta, F., and Haimann, C. (1994) *J. Membr. Biol.* **138**, 91–102
36. Sugita, S., Ichtchenko, K., Khvotchev, M., and Südhof, T. C. (1998) *J. Biol. Chem.* **273**, 32715–32724
37. Longenecker, H. E., Hurlbut, W. P., Mauro, A., and Clark, A. W. (1970) *Nature* **225**, 701–703
38. Ceccarelli, B., and Hurlbut, W. P. (1980) *J. Cell Biol.* **87**, 297–303
39. Elrick, D. B., and Charlton, M. P. (1999) *J. Neurophysiol.* **82**, 3550–3562
40. Tsang, C. W., Elrick, D. B., and Charlton, M. P. (2000) *J. Neurosci.* **20**, 8685–8692
41. Krasnoperov, V., Bittner, M. A., Holz, R. W., Chepurny, O., and Petrenko, A. G. (1999) *J. Biol. Chem.* **274**, 3590–3596
42. Geppert, M., Khvotchev, M., Krasnoperov, V., Goda, Y., Missler, M., Hammer, R. E., Ichtchenko, K., Petrenko, A. G., and Südhof, T. C. (1998) *J. Biol. Chem.* **273**, 1705–1710
43. Tobaben, S., Südhof, T. C., and Stahl, B. (2002) *J. Biol. Chem.* **277**, 6359–6365
44. Liu, J., and Mislis, S. (1998) *J. Neurosci.* **18**, 6113–6125
45. Capogna, M., Volynski, K. E., Emptage, N., and Ushkaryov, Y. A. (2003) *J. Neurosci.* **23**, 4044–4053